

Relaxation time distribution from time and frequency domain dielectric spectroscopy in poly(aryl ether ether ketone)

A. Bello, E. Laredo, M. Grimau, A. Nogales, and T. A. Ezquerra

Citation: *J. Chem. Phys.* **113**, 863 (2000); doi: 10.1063/1.481862

View online: <http://dx.doi.org/10.1063/1.481862>

View Table of Contents: <http://jcp.aip.org/resource/1/JCPSA6/v113/i2>

Published by the [AIP Publishing LLC](http://www.aipublishing.com).

Additional information on *J. Chem. Phys.*

Journal Homepage: <http://jcp.aip.org/>

Journal Information: http://jcp.aip.org/about/about_the_journal

Top downloads: http://jcp.aip.org/features/most_downloaded

Information for Authors: <http://jcp.aip.org/authors>

ADVERTISEMENT



Explore the **Most Cited** Collection in Applied Physics



Relaxation time distribution from time and frequency domain dielectric spectroscopy in poly(aryl ether ether ketone)

A. Bello and E. Laredo^{a)}

Physics Department, Universidad Simón Bolívar, Apartado 89000, Caracas 1080, Venezuela

M. Grimau

Materials Science Department, Universidad Simón Bolívar, Apartado 89000, Caracas 1080, Venezuela

A. Nogales and T. A. Ezquerro

Instituto de Estructura de la Materia, C.S.I.C., Serrano 119, Madrid 28006, Spain

(Received 7 February 2000; accepted 10 April 2000)

A new application of the simulated annealing Monte Carlo procedure is presented and applied to the extraction of the relaxation time distribution from dielectric spectroscopy either in time or frequency domain. This decomposition method named simulated annealing direct signal analysis (SADSA), is applied to computer generated curves, $\epsilon(t)$, $\epsilon'(\omega)$, and $\epsilon''(\omega)$, by using the most widely accepted empirical distributions. The discretized distribution fits exactly the analytical expression which can be evaluated in these cases for the set of parameters used in the simulation. Also, both distribution functions are found to be identical which proves that the method is certainly converging to the right solution in both cases. Experimental results on amorphous poly(aryl ether ether ketone) for $\epsilon(t)$, $\epsilon'(\omega)$, and $\epsilon''(\omega)$ are analyzed with SADSA and the obtained relaxation time distribution is used to go from time to frequency domain and reciprocally. The results are compared to those obtained by assuming a Havriliak–Negami profile for the distribution function. © 2000 American Institute of Physics. [S0021-9606(00)50226-8]

I. INTRODUCTION

There has been a considerable interest in recent time, to find relationships between the conditions which describe the same relaxation process in frequency and in time domain, respectively.^{1–4} In the case of the α or slow relaxation, appearing in glass forming liquids and polymers above the glass transition temperature (T_g), most efforts have been devoted to provide mathematical expressions for these relationships.^{1–5} The extraction of the relaxation time distribution function, $G(\ln(\tau))$, from the variation with time or frequency of a relaxation function, in this case the dielectric function, has been the object of extended work. The expression of the time dependent dielectric constant can be written as

$$\epsilon(t) = \epsilon_U + (\epsilon_R - \epsilon_U)[1 - \phi(t)], \quad (1)$$

where ϵ_R and ϵ_U are the relaxed ($t = \infty$) and unrelaxed ($t = 0$) dielectric constant values and $\phi(t)$ is the macroscopic decay function. In time domain a good description for the decay function is the so-called stretched exponential introduced by Kohlrausch and later on by Williams and Watts (KWW).^{6,7}

$$\phi(t) = \exp[-(t/\tau_{KWW})^\beta], \quad (2)$$

where β varies from 1 (Debye process) to 0 and it characterizes the width of the relaxation time distribution. In term of the distribution of relaxation time, the decay function is expressed as

$$\phi(t) = \int_{-\infty}^{+\infty} G(\ln(\tau)) \exp\left(-\frac{t}{\tau}\right) d \ln(\tau). \quad (3)$$

In the frequency domain, the complex dielectric constant is written for a pure Debye process as a function of the angular frequency, ω , at a given temperature T , as

$$\epsilon^*(\omega, T) = \epsilon_U + \frac{\epsilon_R - \epsilon_U}{1 + i\omega\tau}. \quad (4)$$

If now a distribution of relaxation time is assumed the preceding expression in frequency domain becomes

$$\epsilon^*(\omega, T) = \epsilon_U + (\epsilon_R - \epsilon_U) \int_{-\infty}^{+\infty} \frac{G(\ln(\tau))}{1 + i\omega\tau} d \ln(\tau), \quad (5)$$

with the real and imaginary part of ϵ^* being, respectively,

$$\epsilon'(\omega, T) = \epsilon_U + (\epsilon_R - \epsilon_U) \int_{-\infty}^{+\infty} \frac{G(\ln(\tau))}{1 + \omega^2\tau^2} d \ln(\tau) \quad (6)$$

and

$$\epsilon''(\omega, T) = (\epsilon_R - \epsilon_U) \int_{-\infty}^{+\infty} \frac{G(\ln(\tau))\omega\tau}{1 + \omega^2\tau^2} d \ln(\tau). \quad (7)$$

The most widely used distribution function for the phenomenological description of dielectric experiments is the Havriliak–Negami, HN, expression which describes an asymmetric and broadened profile as compared to a Debye curve, the expression of the complex dielectric constant being now

^{a)}Electronic mail: elaredo@usb.ve

$$\epsilon^*(\omega, T) = \epsilon_U + \frac{\epsilon_R - \epsilon_U}{[1 + (i\omega\tau_{\text{HN}})^\alpha]^\gamma}, \quad (8)$$

where the parameters α and γ are related to the broadening and the asymmetry of the profile, respectively.

The relationship between $\epsilon^*(\omega, T)$ and $\phi(t, T)$ is given by the one-side Fourier or pure imaginary Laplace transformation of the form^{6,7}

$$\frac{\epsilon^*(\omega) - \epsilon_U}{\epsilon_R - \epsilon_U} = \int_0^\infty (-d\phi/dt) \exp(-i\omega t) dt. \quad (9)$$

To obtain the relaxation time distribution function from the experimental data gathered with a variety of techniques which measure the decay function as a function of time, the CONTIN program, proposed by Provencher,⁸ is a procedure widely used in recent works. By means of an inverse Laplace transform the CONTIN code is used to extract $G(\ln(\tau))$ from the decay function⁹ written above [Eq. (3)]. The advantage of the CONTIN procedure is the use of a constraint regularization method which leads to the solution with less structure among the possible solutions. This method has been recently successfully adapted by Alvarez *et al.*⁹ to computer simulated curves, $\epsilon''(\omega)$, with a variety of distribution functions and to experimental data of polyvinylchloride and a liquid crystalline polymer, in the frequency domain.

The simulated annealing direct signal analysis procedure (SADSA) is a new method used to decompose the relaxation spectrum in Debye processes, each of them contributing to the spectrum with a weight according to the profile of the discrete distribution of relaxation time. The details of the computing method have been given elsewhere.¹⁰ The method is based on the simulated annealing Monte Carlo procedure widely used since its introduction by Kirkpatrick *et al.*¹¹ The validity of our procedure in the frequency domain has been tested with computer generated curves based on a variety of distribution functions such as, Cole–Cole, Cole–Davidson, Havriliak–Negami, and KWW.¹⁰ The histograms obtained which describe the discretized distribution functions, are in excellent agreement with the analytical distributions whose expressions are known in the first three cases; for the KWW decay function the corresponding distribution function is known for $\beta=0.5$, for other β values where there is not an exact analytical expression the distribution can be calculated by numerical integration (see expression in Table I of Bello *et al.*¹⁰) to any desired degree of precision. In spite of these theoretical works, experimental work on this topic has been very scarce and restricted to very particular cases.^{2,12}

The aim of the present work is twofold. Firstly, to explore the validity of the SADSA method to obtain the distributions of relaxation time from time domain and frequency domain computer simulated curves. Secondly, to establish a direct correlation between the distribution of relaxation time obtained independently from experimental time domain and frequency domain dielectric results for the case of the α -relaxation of poly(aryl-ether-ether-ketone).

II. EXPERIMENT

Time domain and frequency domain dielectric experiments were performed on amorphous poly(aryl-ether-ether-ketone) (PEEK, 450 G, ICI) which is the customary name of poly(oxy-1, 4-phenyleneoxy-1, 4-phenylenecarbonyl-1, 4-phenylene) with $T_g=418$ K, $M_n \sim 12\,500$ g/mol and $M_w \sim 40\,000$ g/mol. Time domain measurements of the dielectric constant, $\epsilon(t)$, were performed as described elsewhere¹³ from 10^{-6} to 10 s, by using a Mopsik dielectric spectrometer¹⁴ (IMASS Corp., Hingham, MA). Frequency domain measurements of the complex dielectric permittivity, were performed at $12 \text{ Hz} \leq \omega/2\pi \leq 10^5$ Hz with a system (Novocontrol GmbH, Hundsangen, Germany) integrating a SR 830 Lock-in amplifier (Stanford Research Systems, Sunnyvale, CA) with a dielectric interface. In both cases, isothermal measurements were performed in amorphous films 0.005 cm thick with gold sputtered electrodes, 2 to 3 cm in diameter. In order to minimize the error in the temperature reading existing among the two different sample holders, relaxation experiments were performed at similar frequency of maximum loss values of $\sim 10^3$ Hz corresponding to $T=(431.5 \pm 1.5)$ K.

III. COMPUTATIONAL METHOD

The SADSA computer program best fits the experimental data, i.e., $\epsilon'(\omega, T)$, $\epsilon''(\omega, T)$ or $\epsilon(t, T)$, by discretizing the distribution function into a sum of M contributions or bins, each characterized by a relaxation time τ_k and a weight or contribution to the response, G_k . The real and imaginary part of the dielectric function can then be approximated by

$$\epsilon'(\omega, T) = \epsilon_U + (\epsilon_R - \epsilon_U) \sum_{k=1}^M \frac{G_k}{1 + \omega^2 \tau_k^2} \Delta \ln(\tau_k), \quad (10)$$

$$\epsilon''(\omega) = \sum_{k=1}^M \frac{G_k \omega \tau_k}{1 + \omega^2 \tau_k^2} \Delta \ln(\tau_k), \quad (11)$$

and in time domain

$$\epsilon(t) = \epsilon_U + (\epsilon_R - \epsilon_U) \sum_{k=1}^M G_k \left(1 - \exp\left(-\frac{t}{\tau_k}\right) \right) \Delta \ln(\tau_k). \quad (12)$$

The input of the program is a set of M equidistant starting values of τ_k in a chosen interval for $\ln(\tau)$. Initially, all the relaxation processes contribute equally, i.e., the distribution is box-shaped, and if the annealing schedule is appropriate the program will converge to the global minimum of the “energy” due to the random exploration of the parameters’ space. The discretized distribution of relaxation time which best fit the experimental data is obtained as the set of contributions, G_k , of each elementary process.

IV. RESULTS AND DISCUSSION

A. Distribution of relaxation time from computer generated $\epsilon'(\omega, T)$, $\epsilon''(\omega, T)$, and $\epsilon(t, T)$ curves

In order to test the method a set of $\epsilon'(\omega, T)$, $\epsilon''(\omega, T)$, and $\epsilon(t, T)$ were generated assuming a HN distribution func-

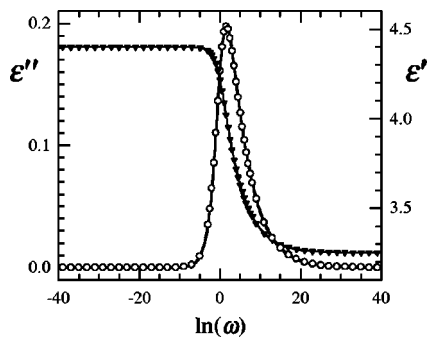


FIG. 1. Computer-generated $\epsilon'(\omega)$ (\blacktriangledown , right vertical axis) and $\epsilon''(\omega)$ (\circ , left vertical axis) with a HN distribution of relaxation time ($\alpha=0.7$, $\gamma=0.3$, $\tau_{\text{HN}}=1$ s). The lines are the results of the best fit achieved with the SADS procedure.

tion. In the frequency domain the generated data is plotted on Fig. 1; the symbols represent the calculated points for $\epsilon'(\omega, T)$ and $\epsilon''(\omega, T)$ ($\alpha=0.7$, $\gamma=0.3$, and $\tau_{\text{HN}}=1$ s, $\Delta\epsilon=1.15$, $\epsilon_U=3.25$) and the continuous line the results of the SADS fitting procedure. The sum of squares residuals, SSR, are $\chi^2_{\epsilon''(\omega)}=8.4 \times 10^{-7}$ and $\chi^2_{\epsilon'(\omega)}=7.2 \times 10^{-6}$ whose low values confirms the visual quality of the fittings. The relaxation time distribution resulting from this analysis is identical in both cases and it is represented in Fig. 2 as a relaxation times histogram, the height of each bar being proportional to the contribution of each elementary process, with relaxation time τ_k , to the complex curve. In this same figure the continuous line represents the analytical expression of the correct expression for the HN distribution¹⁰ which follows very closely the discretized profile

$$G(\ln(\tau)) = \frac{1}{\pi} \frac{\sin(\gamma\theta)}{(1 + 2(\tau/\tau_{\text{HN}})^\alpha \cos(\pi\alpha/2) + (\tau/\tau_{\text{HN}})^{2\alpha})^{\gamma/2}}, \quad (13)$$

with

$$\theta = \frac{\pi}{2} - \tan^{-1} \left(\frac{(\tau_{\text{HN}}/\tau)^\alpha + \cos(\pi\alpha)}{\sin(\pi\alpha)} \right),$$

for $\alpha=0.7$, $\gamma=0.3$, and $\tau_{\text{HN}}=1$ s.

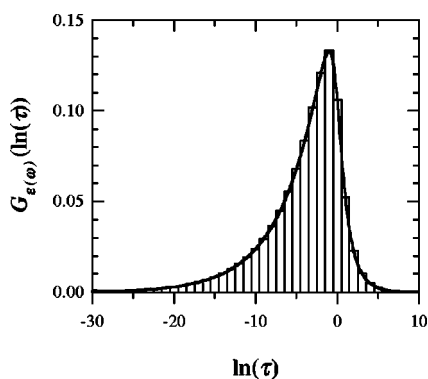


FIG. 2. Distribution of relaxation time from the HN curves represented in Fig. 1. The bar diagram is the discretized $G_{\epsilon(\omega)}(\ln(\tau))$ in frequency domain obtained from either $\epsilon'(\omega)$ or $\epsilon''(\omega)$. The continuous line is the representation of the analytical HN distribution [Eq. (13)] with $\alpha=0.7$, $\gamma=0.3$, $\tau_{\text{HN}}=1$ s.

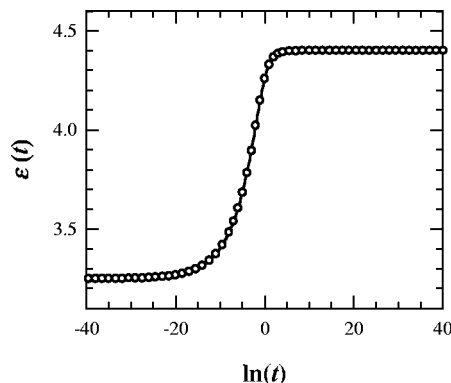


FIG. 3. Computer-generated $\epsilon(t)$ with a HN distribution of relaxation time ($\alpha=0.7$, $\gamma=0.3$, $\tau_{\text{HN}}=1$ s). The line is the result of the best fit achieved with the SADS procedure.

In time domain, the corresponding curves for $\epsilon(t, T)$ are represented in Fig. 3 for the same HN parameters as before. The open symbols are the simulated points calculated by combining Eqs. (13) and (3) to obtain $\phi(t)$ and using Eq. (1) to generate $\epsilon(t, T)$; the continuous line is the best fit of these simulated points to Eq. (12) obtained with the SADS procedure. Here $\chi^2_{\epsilon(t)}=1.1 \times 10^{-5}$ is again very low and the corresponding $G_{\epsilon(t)}(\ln(\tau))$ is plotted on Fig. 4 as a relaxation times histogram. Here again the agreement between the extracted discretized $G_{\epsilon(t)}(\ln(\tau))$ and the analytical HN function [Eq. (13)] is excellent. Additionally, the two independently obtained histograms (Figs. 2 and 4) and consequently the corresponding distribution functions are identical. The above described procedure has been tried for a wide range of α and γ parameters with similar results. The validity of the SADS procedure is then proved to be fully satisfactory when there exist data covering a wide frequency range; the procedure leads to identical distribution functions either from frequency domain data, i.e., $\epsilon'(\omega, T)$ or $\epsilon''(\omega, T)$ or from time domain data, $\epsilon(t, T)$.

B. Distribution of relaxation time from experimental $\epsilon'(\omega, T)$, $\epsilon''(\omega, T)$ curves for the α -relaxation in amorphous PEEK

The experimental $\epsilon''(\omega, T)$ (left vertical axis) and $\epsilon'(\omega, T)$ curves (right vertical axis) obtained for the α -mode

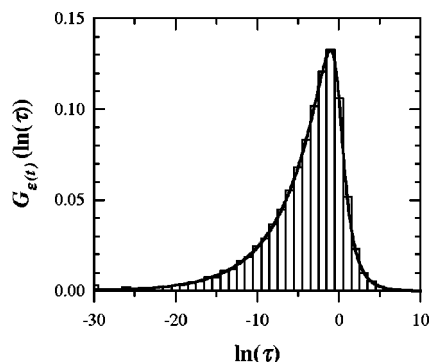


FIG. 4. Distribution of relaxation time from the HN curve for $\epsilon(t)$ represented in Fig. 3. The bar diagram is the discretized $G_{\epsilon(t)}(\ln(\tau))$ in time domain obtained from $\epsilon(t)$. The continuous line is the representation of the analytical HN distribution [Eq. (13)] $\alpha=0.7$, $\gamma=0.3$, $\tau_{\text{HN}}=1$ s.

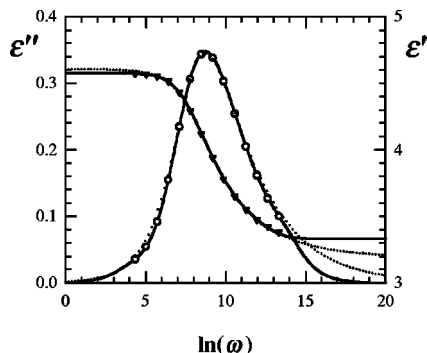


FIG. 5. α -relaxation of amorphous PEEK in frequency domain, $T=431.5$ K: $\epsilon'(\omega)$ (\blacktriangledown , right vertical axis) and $\epsilon''(\omega)$ (\circ , left vertical axis). The continuous lines are the results of the best fit achieved with the SADSA procedure. The dotted lines represent the calculated ϵ' and ϵ'' functions with the parameters from the approximation of the histogram shown on Fig. 6 to a HN distribution.

on PEEK films (symbols) are shown on Fig. 5 for $T=431.5$ K and for $12 \text{ Hz} \leq \omega/2\pi \leq 10^5 \text{ Hz}$. The continuous lines are the result of the SADSA fitting with $\chi^2_{\epsilon''} = 3.2 \times 10^{-7}$ and $\chi^2_{\epsilon'} = 1.0 \times 10^{-6}$. The distribution of relaxation time, $G_{\epsilon''(\omega)}(\ln(\tau))$, obtained from the best fit to the $\epsilon''(\omega, T)$ experimental data is shown in Fig. 6 as a relaxation times histogram (white wide bars). Due to the absence of data for $\omega > 6.3 \times 10^5 \text{ rad/s}$, the short τ values are omitted as the experiment does not record the complete decay of the loss on the high-frequency tail. On Fig. 6 the histogram obtained from the SADSA fitting of $\epsilon'(\omega)$, $G_{\epsilon'(\omega)}(\ln(\tau))$, is represented by narrow bars with a pattern of diagonal lines and it is readily seen that the similarity between the two histograms is excellent. From the fitting of any of the two relaxation time histograms to a HN distribution (see continuous curves in Fig. 6), the characteristic parameters are found to be: $\Delta\epsilon = 1.30$, $\alpha = 0.78$, $\gamma = 0.50$, $\tau_{\text{HN}} = 3.5 \times 10^{-4} \text{ s}$. The calculated $\epsilon''(\omega)$ and $\epsilon'(\omega)$ curves with these HN parameters are shown in Fig. 5 as dotted lines. The observed differences between the SADSA fit and the HN approximation to the relaxation time histogram are significant and can be quanti-

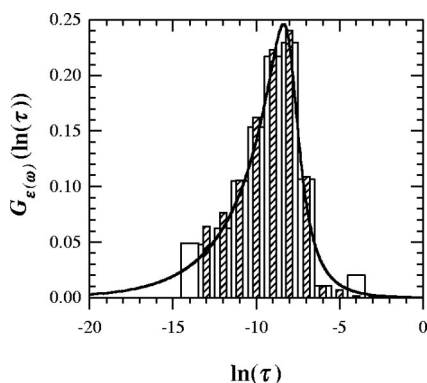


FIG. 6. Distribution of relaxation time in frequency domain for the α -relaxation of amorphous PEEK, $T=431.5$ K: The bar diagram is the discretized: $G_{\epsilon''(\omega)}(\ln(\tau))$ (white bars), $G_{\epsilon'(\omega)}(\ln(\tau))$ (diagonal pattern bars), obtained, respectively, from the best fit of $\epsilon''(\omega)$ and $\epsilon'(\omega)$ shown on Fig. 5. The continuous line is the best fit of the histogram to a HN distribution: $\Delta\epsilon = 1.30$, $\alpha = 0.78$, $\gamma = 0.50$, $\tau_{\text{HN}} = 3.5 \times 10^{-4} \text{ s}$.

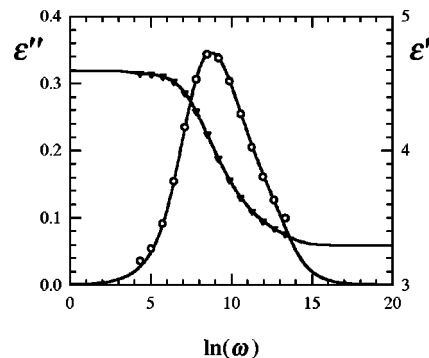


FIG. 7. α -relaxation of amorphous PEEK in frequency domain, $T=431.5$ K: $\epsilon'(\omega)$ (\blacktriangledown , right vertical axis) and $\epsilon''(\omega)$ (\circ , left vertical axis). The lines are the results of the simulation of these functions by using the SADSA distribution of relaxation time $G_{\epsilon''(\omega)}(\ln(\tau))$ to calculate $\epsilon'(\omega)$; $G_{\epsilon'(\omega)}(\ln(\tau))$ to calculate $\epsilon''(\omega)$.

fied by the SSR which is now 5.9×10^{-4} for the fit to $\epsilon''(\omega)$, i.e., three orders of magnitude larger than that found by SADSA. Imposing a HN profile for the distribution leads to an approximation of the experimental results which is not as satisfactory as the SADSA procedure result, even if the general allure of the curve approaches the shape of the HN distribution. A direct fitting of the experimental points $\epsilon''(\omega)$ to the HN expression for the imaginary part of the dielectric constant (see Table 1 in Ref. 10), leads now to the following characteristic parameters, $\Delta\epsilon = 1.37$, $\alpha = 0.81$, $\gamma = 0.45$, $\tau_{\text{HN}} = 3.8 \times 10^{-4} \text{ s}$, $\chi^2 = 6.5 \times 10^{-5}$. The latter differ slightly from those found before,¹³ and the SSR is an order of magnitude lower than previously, but still higher by a factor of 100 than that obtained by the SADSA procedure. The best fitting quality is obtained with the SADSA procedure which has the advantage of finding the best distribution without invoking any imposed profile for the sought distribution. However, it is noteworthy that the assumption of a HN distribution to fit either $\epsilon''(\omega)$ or $G_{\epsilon''(\omega)}(\ln(\tau))$ leads to fittings of acceptable quality as shown by SSR, χ^2 , in the range of 10^{-4} – 10^{-5} . The results obtained by interchanging the distribution function found in the fit of $\epsilon''(\omega, T)$ to generate $\epsilon'(\omega, T)$ and reciprocally, are plotted on Fig. 7 together with the experimental points for PEEK. The continuous curves are the results of the SADSA fittings: The imaginary part of the dielectric constant is calculated with the discrete distribution deduced from the fit of the real part and reciprocally. As can be seen from Figs. 5 and 7 any of the two distribution functions independently found, works equally well to adjust the experimental data of the real or imaginary part of the dielectric function in frequency domain.

C. Distribution of relaxation time from experimental $\epsilon(t, T)$ curves for the α -relaxation in amorphous PEEK

On going now from frequency to time domain, experiments are performed on a similar amorphous PEEK, at the same temperature and over a time interval $10^{-6} \text{ s} < t < 10 \text{ s}$; the results are shown in Fig. 8 (open symbols). It is to be noted that the steep increase of the dielectric constant for longer times, due to the conductivity contribution has been

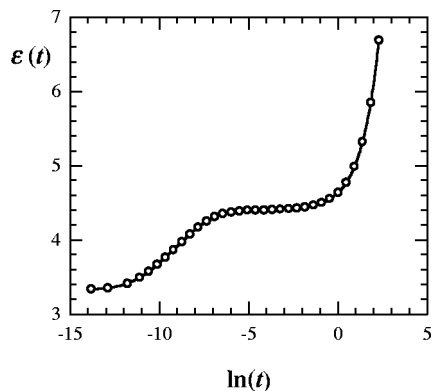


FIG. 8. α -relaxation of amorphous PEEK in time domain, $T=431.5$ K: $\epsilon(t)$ (\circ) experimental points. The line is the result of the best fit achieved for the distribution of relaxation time $G_{\epsilon(t)}(\ln(\tau))$ with the SADSA procedure. $\Delta\epsilon = 1.09$, $\epsilon_U = 3.32$, $b = 0.23$.

taken into account by adding to Eq. (12) a term bt , where b is assumed constant. The discretized distribution of relaxation time, obtained from the best SADSA fit to the experimental data, is represented on Fig. 9 ($\epsilon_U = 3.32$, $\Delta\epsilon = 1.09$, $b = 0.23$ s $^{-1}$). Due to the limited time range of the data, mainly at low times, there appears a lack of contributions for $\tau \leq 10^{-12}$ s, which consequence is the absence of a smooth decay of $G_{\epsilon(t)}(\ln(\tau))$ distribution at short τ .

To compare the distributions obtained either in frequency or time domain, $\epsilon''(\omega)$ is calculated and shown in Fig. 10 (left vertical axis), by using the discrete $G_{\epsilon(t)}(\ln(\tau))$ obtained in time domain. The agreement between the calculated curve (dotted line) and the experimental data (open circles) is satisfactory at low frequencies. At higher frequencies the tail of the experimental curve is wider due to the lack of experimental $\epsilon(t)$ data at short times which in turn is responsible for the absence of significant contributions, G_k , at low $\ln(\tau)$ values in the histogram shown on Fig. 9. On the other hand, the simulation of the real part, $\epsilon'(\omega)$, of the dielectric constant with the discrete $G_{\epsilon(t)}(\ln(\tau))$ represented on the same Fig. 10 (filled triangles, right vertical axis, and dotted line), shows a better agreement than that found for the imaginary part.

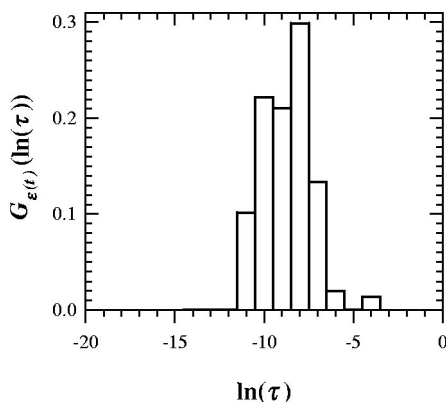


FIG. 9. Distribution of relaxation time in time domain for the α relaxation of amorphous PEEK, $T=431.5$ K: The bar diagram is the discretized $G_{\epsilon(t)}(\ln(\tau))$ obtained from the best fit of $\epsilon(t)$ shown on Fig. 8.

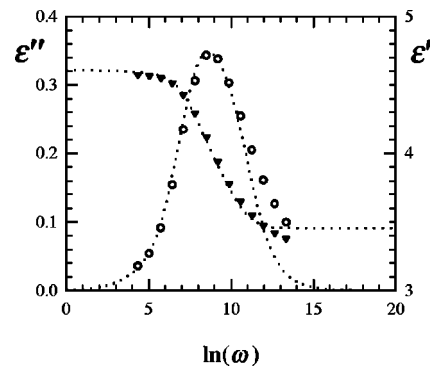


FIG. 10. α -relaxation of amorphous PEEK in frequency domain, $T = 431.5$ K: $\epsilon'(\omega)$ (\blacktriangledown , right vertical axis) and $\epsilon''(\omega)$ (\circ , left vertical axis). The lines are the results of the simulation of these functions by using the distribution of relaxation time $G_{\epsilon(t)}(\ln(\tau))$ (Fig. 9) to calculate $\epsilon'(\omega)$ and $\epsilon''(\omega)$.

A similar comparison can be carried out now in time domain, i.e., calculate $\epsilon(t)$ either with the discrete $G_{\epsilon'(\omega)}(\ln(\tau))$ or $G_{\epsilon''(\omega)}(\ln(\tau))$ obtained in frequency domain and shown on Fig. 6. The results appear now on Fig. 11, and again the agreement is very satisfactory. The fitting is made by taking the discrete distribution profile and generating the dielectric function in time domain by means of expression (12). Additionally, the values of $\epsilon_U = 3.14$, $\Delta\epsilon = 1.26$, $b = 0.23$ s $^{-1}$ are found, which compare well to those reported above from the fitting of $\epsilon(t)$ with $G_{\epsilon(t)}(\ln(\tau))$.

Summing up the results obtained on amorphous PEEK for the α -relaxation, it has been shown that the SADSA procedure does not require to decide *a priori* neither the number of overlapping broadened processes, nor the profile of $G(\ln(\tau))$, as it is the case in most currently commercially available software. On the contrary, the obtained relaxation time histogram can be fitted to any chosen profile as it has been done in the present work for HN distributions with reasonable results. The validity of the distribution of the relaxation time, extracted either in frequency or in time domain, to predict the variation of $\epsilon''(\omega, T)$ or $\epsilon'(\omega, T)$ and $\epsilon(t, T)$, has been proved. The knowledge of one of these functions allows the simulation of the others.

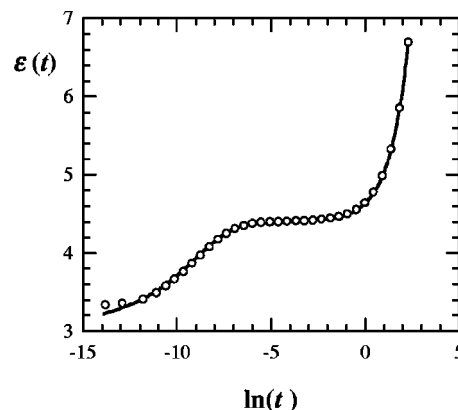


FIG. 11. α -relaxation of amorphous PEEK in time domain, $T=431.5$ K: $\epsilon(t)$, the line is the result of the simulation of this function by using the distribution of relaxation time $G_{\epsilon'(\omega)}(\ln(\tau))$ or $G_{\epsilon''(\omega)}(\ln(\tau))$ shown on Fig. 6.

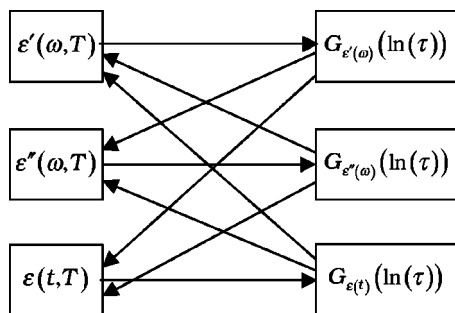


FIG. 12. Schematic summary of the various paths used to calculate the dielectric functions $\epsilon'(\omega)$, $\epsilon''(\omega)$, and $\epsilon(t)$ with the distribution functions obtained with SADS procedure for the α -relaxation of amorphous PEEK.

V. CONCLUSIONS

A new method proposed here to calculate the relaxation time distribution from dielectric spectroscopy data has been shown to work both on computer generated curves and experimental data in frequency and time domain. The agreement and resolution of the spectra is very satisfactory in the cases tested by us which cover the most frequently used distribution functions. The obtained distribution functions from frequency domain can be used to simulate the dielectric data in time domain and reciprocally. In Fig. 12 the various tests of the distribution function determination by switching from frequency to time domain and reciprocally have been represented. When the SADS procedure is applied to experimental data the fit of the curves is excellent even though the limited time range introduces some distortion in the tails of the function. In this way, one can predict $\epsilon''(\omega)$ or $\epsilon'(\omega)$ when working in time domain or $\epsilon(t)$ if the variable is the angular frequency. The various methods used previously have not been tested both in time and frequency domain. The SADS procedure has been shown to extract precisely the distribution function from either $\epsilon''(\omega)$, $\epsilon'(\omega)$ or $\epsilon(t)$. It is important to note that the SADS procedure always leads here to the best quality fittings, and the profile of the distribution function is always close to a HN function, but the SADS can reveal fine structure details which will be ignored if a profile is *a priori* imposed. The main advantage of the SADS is when the situation is not that simple and the experimental curve results from the overlap of several relaxation processes. The relaxation time distribution that best fits the experimental points is determined without any assumption on the number, or the characteristic parameters of overlapping distributed modes. With the discrete distribution obtained by applying the SADS to any domain one can a posteriori, intent a separation of the different processes. The importance of the precise knowledge of $G(\ln(\tau))$ to estimate the decay function from the widespread dielectric spectroscopy in frequency domain has been shown in many previous works. A somewhat similar approach has been taken by Bergman *et al.*¹⁵ to estimate the decay function $\phi(t)$ from measurements in ω domain. They use a modified CONTIN algorithm acting in frequency domain, to extract $G(\ln(\tau))$

from $\epsilon''(\omega)$. They show that the knowledge of the decay function in the case of syndiotactic PMMA allows the detailed study of the merging of the α and β relaxations which is explained in terms of Williams' ansatz without any need to appeal to a change in the chain dynamics in the merging region. The statistical independence assumed for the α and β processes in a main chain glass forming polymer is a controversial result.^{16,17} Many other conclusions can be reached from the detailed knowledge of $G(\ln(\tau))$ when analyzing the variations induced in the relaxation spectra by changing the specimen preparation. Karatasos *et al.*¹⁸ have shown in diblock copolymers, that the differences observed in samples prepared from the melt and by slow solvent casting are related to the coherence of the ordered structure. Also the variation of the width of the distribution, which shows a broadening as compared to that of the homopolymer when the temperature is decreased and/or the molecular weight increased, are attributed by these authors to composition fluctuations and proximity to the glass transition effects on the normal mode relaxation. The transformation of $G(\ln(\tau))$ to the decay function is also very useful as the number of overlapping relaxations is best determined by fitting the decay function to several KWW functions. The SADS provides an easy way to switch to time domain where a number of models need extensive test.

ACKNOWLEDGMENTS

Financial support from the Consejo Nacional de Investigaciones Científicas y Tecnológicas (CONICIT G97-000594) is gratefully acknowledged. T.A.E and A.N. are indebted to Comunidad de Madrid (07N/0063/1998) and to DGICYT (Grant No. PB 94-0049) Spain, for partial support of this investigation. A.N. thanks the support from the FPI program of the Spanish Ministry of Science and Culture (MEC).

- ¹R. H. Boyd, R. W. Devereaux, and R. B. Thayer, *Polym. Prepr. (Am. Chem. Soc. Div. Polym. Chem.)* **31**, 279 (1990).
- ²F. Alvarez, A. Alegria, and J. Colmenero, *Phys. Rev. B* **44**, 7306 (1991).
- ³S. Havriliak, Jr. and S. J. Havriliak, *Polymer* **36**, 2675 (1995).
- ⁴S. Havriliak, Jr. and S. J. Havriliak, *Polymer* **37**, 4107 (1996).
- ⁵F. Alvarez, A. Alegria, and J. Colmenero, *Phys. Rev. B* **47**, 125 (1993).
- ⁶G. Williams and D. C. Watts, *Trans. Faraday Soc.* **66**, 80 (1970).
- ⁷M. Cook, D. C. Watts, and G. Williams, *Trans. Faraday Soc.* **66**, 2503 (1970).
- ⁸S. W. Provencher, *Comput. Phys. Commun.* **27**, 213 (1982).
- ⁹F. Alvarez, A. Alegria, and J. Colmenero, *J. Chem. Phys.* **103**, 798 (1995).
- ¹⁰A. Bello, E. Laredo, and M. Grima, *Phys. Rev. B* **60**, 12764 (1999).
- ¹¹S. Kirkpatrick, C. D. Gelatt, Jr., and M. P. Vecchi, *Science* **220**, 671 (1981).
- ¹²D. Boese, B. Momper, G. Meier, F. Kremer, J. U. Hagenah, and E. W. Fischer, *Macromolecules* **22**, 4416 (1989).
- ¹³T. A. Ezquerro, F. Liu, R. H. Boyd, and B. H. Hsiao, *Polymer* **38**, 5793 (1997).
- ¹⁴F. I. Mopsik, *Rev. Sci. Instrum.* **55**, 79 (1984).
- ¹⁵R. Bergman, F. Alvarez, A. Alegria, and J. Colmenero, *J. Chem. Phys.* **109**, 7546 (1998).
- ¹⁶F. Alvarez, A. Hoffman, A. Alegria, and J. Colmenero, *J. Chem. Phys.* **105**, 432 (1996).
- ¹⁷E. Donth, K. Schröter, and S. Kahle, *Phys. Rev. E* **60**, 1099 (1999).
- ¹⁸K. Karatasos, S. H. Anastasiadis, A. N. Semenov, G. Fytas, M. Pitsikalis, and N. Hadjichristidis, *Macromolecules* **27**, 3543 (1994).